Methane-Air Combustion Gases as an Aerodynamic Test Medium

R. R. HOWELL* AND L. R. HUNT†
NASA Langley Research Center, Hampton, Va.

The present paper gives a review of the major problems associated with the use of hydrocarbon-air combustion gases as an aerodynamic test medium. Condensation of water vapor is identified as the major problem, and actual experience is offered as evidence of its effects on aerodynamic flow parameters. Aerodynamic data obtained from tests in methane-air combustion gases are compared with theory and with data obtained on the same shapes in other test facilities using other test media. The comparisons indicate that data obtained in combustion gas compare well with data obtained in other test media.

Nomenclature

A = cross-sectional area
C_A = axial-force coefficient, axial force/q S
C_D = drag coefficient, drag/q S
$C_{L\alpha}$ = slope of the lift curve at $\alpha = 0$
C_m = pitching-moment coefficient, pitching moment/q Sl
C_N = normal-force coefficient, normal force/q S
C_p = specific heat at constant pressure
d = model diameter, cm
l = characteristic length (model length)
M = Mach number
$N_{Re,2}$ = Reynolds number based on the conditions behind normal shock and the model diameter
N_{Re}/L = unit Reynolds number, m^{-1}
N_{Re} = Reynolds number based on the freestream conditions and model length
p = pressure, atm
q = dynamic pressure
$\dot{q}$ = convective heating rate, W/m^2
R = specific gas constant
R_{eq} = equivalence ratio
r = model nose radius, cm
S = characteristic area ($\pi d^2/4$ for spheres, $l^2 \tan\theta$ for cones, and wing area for AGARD Calibration Model B)
s = surface streamline length, cm; or entropy
T = temperature, °K
x = mole fraction
x_{cp} = distance along model center line from the apex to the center of pressure
θ = angle of attack, deg
γ = ratio of specific heats
ρ = density
θ = cone semivertex angle, deg

Subscripts

o = local condition without condensation
s = model stagnation-point condition
t = total (stagnation) condition
w = model wall condition
1 = wind-tunnel nozzle
2 = behind normal shock

Superscript

* = throat (sonic point) condition

Presented as Paper 71-258 at the AIAA 6th Aerodynamic Testing Conference, Albuquerque, N. Mex., March 10–12, 1971; submitted April 5, 1971; revision received August 27, 1971.
Index category: Research Facilities and Instrumentation.
* Head, High Temperature Structures Branch.
† Aerospace Technologist, Structural Cooling Section.

Introduction

THE experimental study of certain hypersonic aircraft and boost vehicle problems requires large hypersonic test streams having realistic energy levels. The mass flow required for realistic simulation of hypersonic flight conditions in such cases is quite large and, as a consequence, the methods available to produce the desired stream energy levels are limited. Methods of solution to the problem of simulation of flight up to $M = 7$ are 1) electric resistance heaters to heat nitrogen used for synthetic air, 2) electric arc air heaters, 3) ceramic heat storage systems, and 4) combustion processes. Each of the approaches has its disadvantages when viewed from the operational, cost, and use standpoints. The least restrained is the combustion process. Energy simulation for $M = 7$ can be obtained by burning an inexpensive hydrocarbon fuel such as methane. The stream temperature is adjustable during the operation by variation of the amount of fuel being burned and the length of the test interval for this case is limited only by the storage volume of fuel and air. The use of combustion gases as an aerodynamic test medium has been generally considered undesirable because the fluid mechanics of the gas mixture has been uncertain and difficult to handle theoretically.

During the past decade the NASA Langley Research Center has developed and placed in operation the Langley 8-ft, high-temperature structures tunnel (a large $M = 7$ blowdown type wind tunnel) which uses methane-air combustion to achieve the gas energy level for flight simulation. This facility was designed to test structures and thermal protection systems for hypersonic aircraft. Hence, problems associated with the fluid mechanics of the gas were considered as secondary.

A large amount of aerodynamic heating, loading, force and moment data has been accumulated from tests in methane-air combustion gases for a variety of body shapes including spheres, cones, hemisphere cylinders and the AGARD Calibration Model B. Concurrently, the advent of large electronic computers has alleviated, to a large extent, the problem of handling the theoretical computations for gas mixtures. The present paper presents a review of the major problems associated with the use of combustion gases as an aerodynamic test medium and summarize scertain comparisons made between experimental aerodynamic data, theory, and data from other facilities using different test media including air.

Discussion of Methane-Air Combustion Gases

The reaction of methane (CH_4) with air produces a gas with molecular constituents of CO_2, H_2O, N_2, and O_2. The mass fraction of the constituents varies with the amount of fuel reacted (see Table 1). Equivalence ratio R_{eq} is a term

Table 1 Equilibrium mole constituency of methane-air combustion gases at various equivalence ratios

	$T = 300°K$		$p = 1$ atm	
R_{eq}	0	0.5	0.8	1.0
N_2	0.7811	0.7353	0.7139	0.6986
O_2	0.2095	0.0974	0.0363	0
CO_2	0	0.0500	0.0776	0.0940
H_2O	0	0.0999	0.1552	0.1859
Ar	0.0093	0.0088	0.0085	0.0083

commonly used to describe the fuel-oxidizer (or fuel-air) mixture. It is defined as:

$$R_{eq} = \frac{\text{ratio of fuel to air}}{\text{ratio of fuel to air for stoichiometric reaction}}$$

Hence, equivalence ratio of 1.0 corresponds to stoichiometric conditions. Equivalence ratios less than 1.0 are fuel lean. In general, for the operation of test facilities, fuel lean conditions are preferred for reasons of safety and cleanliness (avoids carbon deposition) and because the constituency and characteristics of the gas can be more exactly defined. The thermodynamic, transport, and flow properties of fuel lean methane-air mixtures have been computed, for a wide range of gas temperatures and pressures.[1]

At high temperature, the CO_2 and H_2O in the combustion gas dissociate to some extent, depending upon the temperature and pressure. However, even at a relatively low pressure of 1 atm, which is representative of the pressure in the stagnation (behind the bow shock) region on a body, the dissociation is small and should not constitute a problem for aerodynamic studies if properly accounted for.

Vibrational Energy and Relaxation

The presence of the carbon dioxide and water vapor in a test medium gives rise to the possibility of thermal non-equilibrium properties different from those of air under similar conditions. This could affect the instantaneous values of specific heats and the ratio of specific heats. This problem has been studied by a number of persons.[2,3] In the more recent study by Templemeyer[2] it was concluded that the energy distribution mismatch resulting from the CO_2 and H_2O constituents in an oxygen deficient gas is offset by a change in relaxation time such that the product of relaxation time and specific heat due to vibration is about equal to the same product for air. This product of relaxation time and specific heat due to vibrational energy was indicated by Chapman[3] to be more important in describing the effect of energy distribution mismatch on the aerodynamics of the stream than either the discrete value of relaxation time or specific heat alone. The studies that have been made for CO_2 and H_2O constituency levels approximating those in the present combustion gases have indicated that the effect of vibration lag should not constitute a problem with the aerodynamic studies conducted in such a gas.

Condensation of Water Vapor

A more important problem associated with using hydrocarbon-air combustion gases as an aerodynamic test medium is the one arising from the possible condensation of the water vapor as the static temperature of the stream is decreased by the acceleration of the gas in the tunnel nozzle. The energy release associated with the condensation of water can be significant and can cause marked changes in the characteristics of the stream. A number of investigators have probed this problem.[4–7] The degree to which condensation occurs, and the extent to which it modifies the nozzle flow characteristics, is dependent upon the stagnation state of the gas before expansion and the configuration and area ratio of the nozzle. The static pressure and temperature of methane-air combustion gases as developed in a hypersonic nozzle having an area ratio of 230 are presented in Fig. 1 for different stagnation pressure levels and for equivalence ratios of 0.8 and 0.5. The total temperatures for equivalence ratios of 0.8 and 0.5 are 2000°K and 1475°K, respectively. The temperature at the end of the nozzle is indicated. Curves indicating the water vapor saturation temperature and saturation temperature minus 60°K, which has been established as a maximum supercooling that can be obtained in supersonic nozzles, are also shown in the figure. Note that for equivalence ratio of 0.8 the gas in the nozzle achieves the saturation temperature but not the 60°K supercooling. For equivalence ratio 0.5, the static temperature at the nozzle exit is below both the saturation temperature and the 60°K supercooling line. Based on previous experience, it would be expected that at an equivalence ratio of 0.8 the likelihood of condensation should be marginal, whereas at an equivalence ratio of 0.5 condensation should occur.

Inasmuch as the degree of condensation has been found to be unpredictable, calculations of changes in flow parameters due to condensation were made assuming that all of the water water vapor condenses. A comparison of the computed changes in flow parameters for this maximum-condensation case with actual measured values gives an indication of whether condensation exists and the extent of its effect. Some results are shown in Fig. 2 as ratios of the value of a parameter with condensation to its value without condensation along the nozzle center line. The change of state of the water vapor was assumed to occur discontinuously (over zero distance) as indicated by the vertical portions of the curves which indicate the change in parameters due to condensation.

Figure 2a indicates that at an equivalence ratio of 0.8 significant changes in the parameters should result if total condensation occurred. Note that the experimental values are within 2% of the values without condensation indicating apparently condensation-free flow at this equivalence ratio.

Data for an equivalence ratio of 0.5 are presented as Fig. 2b where flow parameter changes are indicated for condensation at both the saturation temperature point and the 60°K supercooled point. It is observed that the further upstream condensation occurs, the smaller the change in the flow

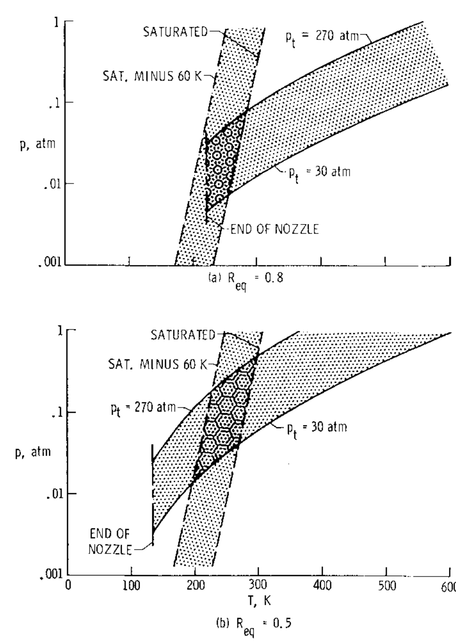

Fig. 1 Saturation conditions for water vapor in methane-air combustion gases compared with conditions developed by the expansion of the gases in a hypersonic nozzle having an A/A^* of 230.

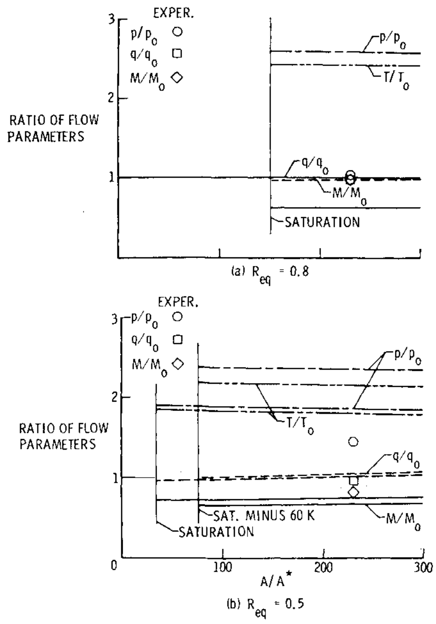

Fig. 2 Ratio of flow parameters with effect of water vapor condensation to those without condensation for methane-air combustion gases when expanded in a nozzle from $p_t = 68$ atm.

parameters. At this equivalence ratio the experimental data appear to reflect some effect of condensation. The measured increase in static pressure is approximately 45% as compared to 90–130% rise for total condensation. The measured Mach number decrease was about 18%, and the measured dynamic pressure difference was about 4%.

From examining these data, it is concluded that when about 60°K supercooling is attained in the nozzle some measurable effects of condensation can be expected. However, condensation, has very little effect on dynamic pressure and the dynamic pressure is the most important flow quantity for aerodynamic studies.

Flow Characteristics of the Stagnation Region

In computing the theoretical heating and loading distributions over blunt bodies immersed in combustion gas flowing at hypersonic speed, particular attention must be paid to accurately defining the conditions at the stagnation point of the body. The pressure and temperature in this region define the entropy level of the gas and, consequently, the transport and flow properties of the gas downstream along the body streamlines. Figure 3 is a Mollier type diagram for methane-air combustion gases for an equivalence ratio of 0.8. A typical variation of the state of the gas along the stagnation streamline is indicated. From the end of the combustion process at p_{t_1} the flow is expanded using a constant entropy process to the test stream conditions at p_∞. Any effects of condensation would appear on this plot as a gain in entropy between p_{t_1} and p_∞. As previously discussed, when condensation is present the value of flow parameter sat the nozzle exit will be different from those defined by an isentropic process, and an experimental calibration is required to properly define the test stream.

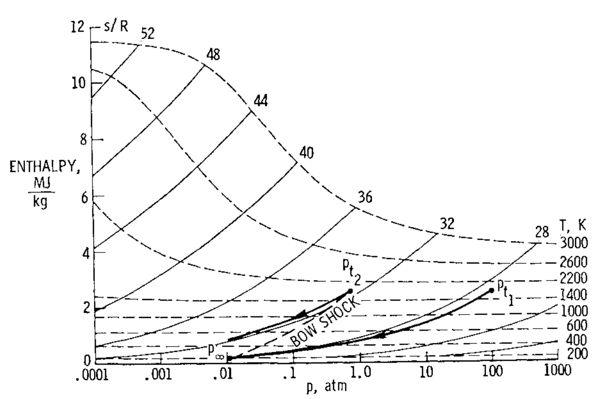

Fig. 3 Mollier diagram showing properties of methane-air combustion gases at $R_{eq} = 0.8$ with a typical stagnation streamline flow indicated.

A major gain in entropy occurs across the body bow wave; this new entropy level, which is established by the inclination of the shock, is maintained in expanding flow until another compression wave or entropy gain is encountered. Because of the sensitivity of the thermodynamic and transport properties of combustion gases to pressure and temperature, the gas must be considered to be a real gas and the instantaneous values of the properties must be used in integral equations to define the local flow. For the range of stream enthalpy required for the simulation of Mach numbers up to about 7, the sensible temperature at the stagnation point is equal to the total temperature of the stream, that is, there is negligible energy in dissociation. Model stagnation-point pressure predicted by theory is not affected significantly by condensation.[7] Hence, nozzle calibrations with pitot surveys should provide an accurate indication of the stagnation-point pressure for bodies in the undisturbed stream.

Methane-Air Combustion-Gas Test Facilities

The facilities used to obtain the experimental results discussed in the following section are the Langley 8-ft, high-temperature structures tunnel and the 7-in. Mach 7 pilot tunnel. These facilities are hypersonic blowdown tunnels in which the high-energy level for $M = 7$ flight simulation is obtained by burning a mixture of methane and air within a pressurized combustion chamber. The resulting combustion gas is expanded through a conical-contoured nozzle to obtain the velocity for simulation. The tunnel stagnation temperature is determined from the output of thermocouple probes inside the combustion chamber just upstream of the nozzle throat contraction. The stagnation temperature is controlled by regulating the fuel-air ratio. The theoretical maximum flame temperature is about 2250°K and is sufficient to simulate the Mach 7 flight environment between about 25 and 40 km altitude.

Discussion of Experimental Aerodynamic Data

Pressure data presented were determined from the output of electrical pressure transducers with the proper pressure ranges for each application. Heating rates presented are for a cold wall and were determined using the output history of thermocouples attached to a thermally thin skin. Force and moment data were determined from the output of strain-gage balances which were internally mounted or shielded. Corrections were made to adjust the base pressure to freestream static pressure for all force data.

Stagnation-Point Heating Rates

Stagnation-point heating for hemispheres as computed by the method of Fay and Riddell[7] is compared with experimentally measured values in Fig. 4. The difference between the theoretical and experimental heating rate is small and generally within experimental accuracy. The comparison indicates that, if the stream conditions are known and if proper values of the thermodynamic and transport properties are used for the combustion gases, blunt-body stagnation heating rates can be accurately predicted.

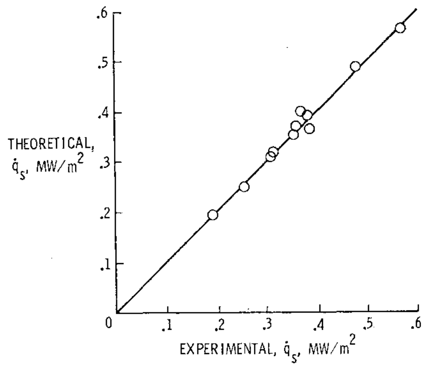

Fig. 4 Comparison of theoretical and experimental stagnation-point heating rates on 30.5 cm diam hemisphere-cylinder model in methane-air combustion gas ($M = 7.3 - 7.9$, $N_{Re}/L - 1.2 - 6.5 \times 10^6\ m^{-1}$).

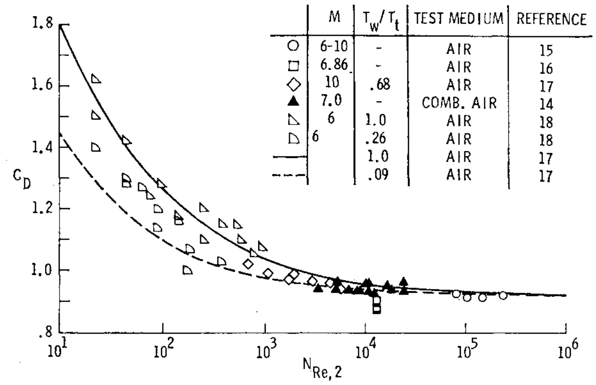

Fig. 6 Variation of sphere drag force coefficient with Reynolds number based on flow conditions behind normal shock at hypersonic Mach numbers.

Heating and Loading Distributions

The experimental pressure and heating rate distributions over a hemisphere cylinder as obtained in methane-air combustion gas are compared with data obtained in air and with theory in Fig. 5. The air data[9-11] in Fig. 5a are for Mach numbers from 4.6–8.0. The theoretical pressure distribution was determined by the method of characteristics with the numerical procedure of Lomax and Inouye[12] using specific combustion gas properties. Over the hemispherical nose the data are all in excellent agreement. Some scatter over the cylinder is expected because of the difference in stream Mach number. The magnitude of the scatter shown is small and generally within the accuracy of experiments (note the log scale on the ordinate).

The heating-rate distributions along hemisphere cylinder models as measured in methane-air combustion gases for different model sizes are compared with theory in Fig. 5b. The theoretical heating distribution was determined by the method of Kemp, Rose, and Detra,[13] using combustion gas properties. The predicted distribution and the experimental data are in good agreement.

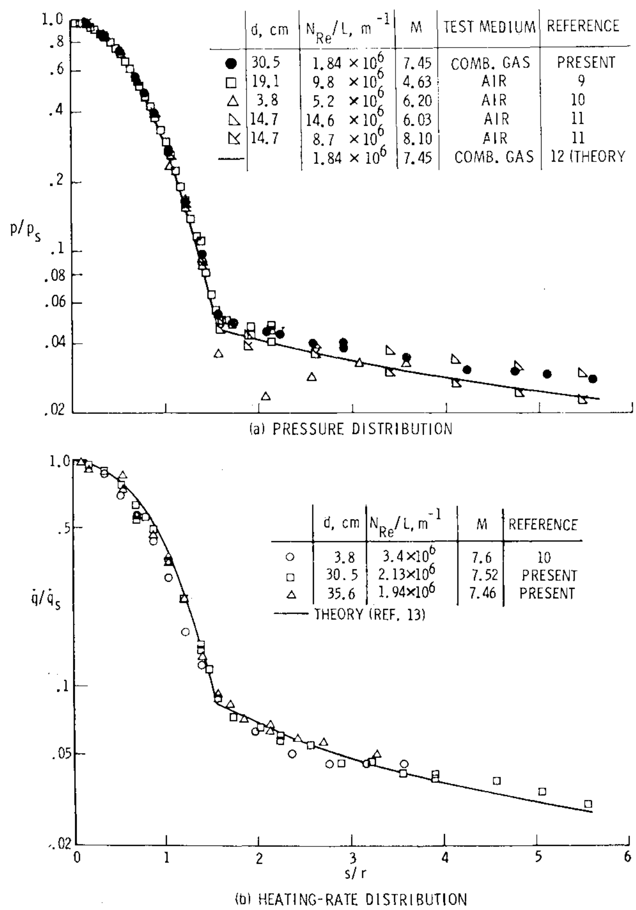

Fig. 5 Variation of pressure and heating along hemisphere-cylinder models as obtained in air and methane-air combustion gas.

Drag Coefficients of Spheres

Drag coefficients as determined for small sting-supported spheres of various diameters tested in methane-air combustion gases[14] are compared with data obtained in air in Fig. 6. The Reynolds number range covered by the combustion gas is near the regime where slip flow is encountered. Hence, the drag coefficient comparison is made as a function of Reynolds number as defined by conditions behind the bow wave. The curves on the figure are those of Kinslow and Potter,[17] representing empirically determined equations for the variation in sphere drag with local Reynolds numbers. The combustion gas data agree well with the predicted curves and with the air data.

Aerodynamic Forces and Moments on Cones

Normal, axial, and pitching-moment coefficients for small sting-supported cones as determined in methane-air combustion gas are presented as a function of angle of attack in Fig. 7. The combustion gas data are compared with data obtained in air and helium[19-21] and with Newtonian theory. In this comparison, there is no large difference in Reynolds number, and the data can be compared directly. The agreement of the data presented in Fig. 7 is considered excellent.

AGARD Calibration Model B

Force and moment data from small-scale tests of the AGARD Calibration Model B are presented in Figs. 8 and 9. All data were obtained in air except the combustion gas data (closed symbols). It is observed in Fig. 8 that the combustion gas data cover a wide range of $M/(N_{Re})^{1/2}$ and extends into the range of possible slip flow ($0.01 < M/(N_{Re})^{1/2} < 1.0$). Below a value of $M/(N_{Re})^{1/2}$ of 0.01, where the bulk of the existing air data fall, the combustion gas data fall within the scatter of other data. It appears that the trend of increasing drag coefficient with increasing values of $M/(N_{Re})^{1/2}$ as indicated by the $M = 8$ air data is supported by the combustion gas data. Lift curve slope, $C_{L\alpha}$, and center-of-pressure location, x_{cp}/d, are presented as a function of Mach number in

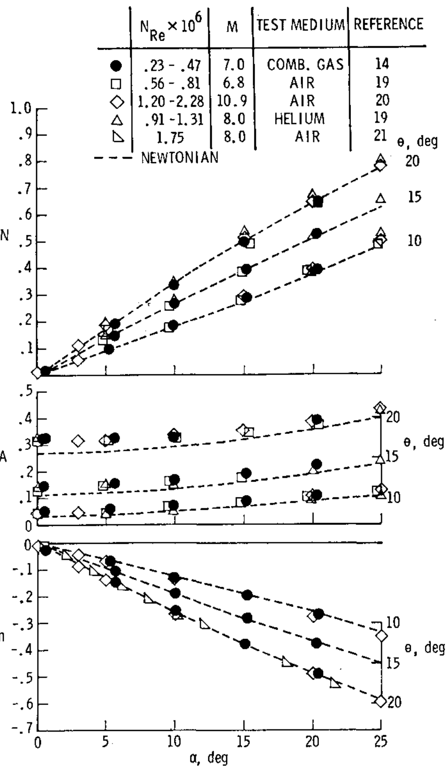

Fig. 7 Variation of force and moment coefficients with angle of attack for sharp nose cones of semivertex angles of 10°, 15°, and 20°.

Fig. 9. In this figure, summary data from ten sources are compared. It is of interest to note that data from all ten sources agree quite well. The combustion products data were plotted at values of Mach numbers determined by assuming isentropic condensation-free flows. The scatter observed in the data reflect a possible effect of condensation on stream Mach number. The data point nearest the drawn curve was obtained at a total temperature of 1830°K and, hence, should be free from condensation effects. The farthest point from the curve (the flagged symbol) was obtained in a test at a total temperature of 1560°K ($R_{eq} \sim 0.5$) and, consequently, should have experienced condensation. If the experimentally determined Mach number for equivalence ratio of 0.5 ($M = 6.2$) (see Fig. 2) is used to plot the data point rather than the Mach number computed for isentropic condensation-free expansion of the gas, the data would fall much closer to the drawn curve. It is clear that, although condensation has only a small effect on dynamic pressure, which is the principle aerodynamic stream parameter at hypersonic speeds, it can

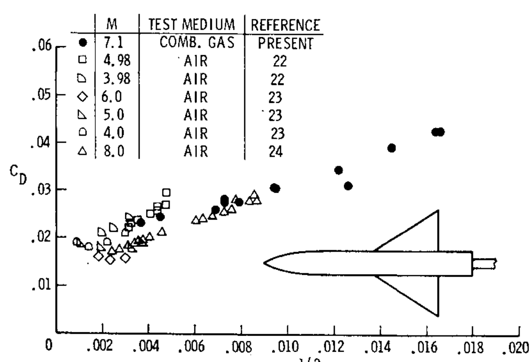

Fig. 8 Variation of drag coefficient with $M/(N_{Re})^{1/2}$ parameter for AGARD calibration model B at zero angle of attack.

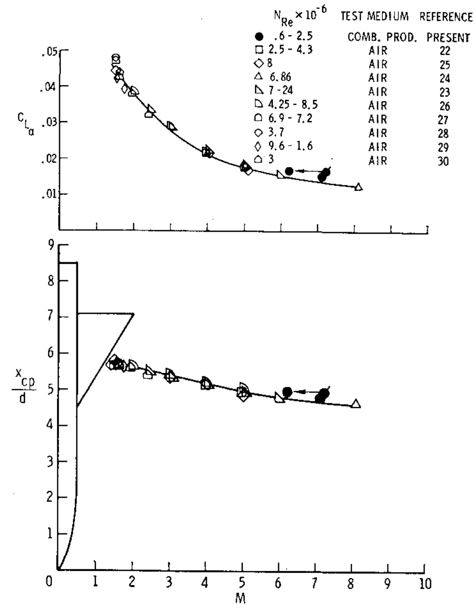

Fig. 9 Variation of $C_{L\alpha}$ and center-of-pressure with Mach number for the AGARD calibration model B.

have a significant influence on Mach number sensitive parameters. Consequently, when using combustion gases where condensation can occur, a detailed experimental calibration of Mach number in the test region as a function of equivalence ratio is required so that accurate Mach number effects are accounted for. If this step is taken, the aerodynamic characteristics of bodies as defined by tests in methane-air combustion gases appear to compare well with those obtained in other gases including air.

Conclusion

A review of the principal problems associated with the use of hydrocarbon-air combustion gases as an aerodynamic test medium is given. It is indicated that condensation of water vapor can have a significant effect on the test flow parameters for methane-air combustion gases at equivalence ratios less than 0.8. However, dynamic pressure, the principal flow parameter at hypersonic speeds, is changed only slightly by condensation. A summary of aerodynamic data on several body shapes as obtained in methane-air combustion gases is presented and compared with theory and with other data obtained on the same shapes in other test facilities and in other test media. The data obtained in the combustion gas compared well with the data obtained in other test media. It is noted that where testing is done in the presence of condensation, Mach number must be determined from experimental static and pitot pressure surveys.

References

[1] Leyhe, E. W. and Howell, R. R., "Calculation Procedure for Thermodynamic, Transport, and Flow Properties of the Combustion Products of a Hydrocarbon Fuel Mixture Burned in Air With Results for Ethylene Air and Methane-Air Mixtures," TN D-914, Jan. 1967, NASA.

[2] Templemeyer, K. E., "An Analytical Study of the Use of Air Equivalent Hot Gaseous Mixtures for Aerodynamic Test Purposes," TN-59-8, March 1959, Arnold Engineering Development Center, Tullahoma, Tenn.

[3] Chapman, D. R., "Some Possibilities of Using Gas Mixtures Other than Air in Aerodynamic Research," TR 1259, 1956, NACA.

[4] Lukusiewiez, J., "Humidity Effects in Supersonic Flow of Air," Rept. Aero 2211, SD 20, July 1947, Royal Aeronautical Establishment, Farnborough, England.

[5] Burgess, Warren C. and Seashore, Ferris L., "Criterion for Condensation-Free Flow in Supersonic Tunnels," TN 2518, Dec. 1951, NACA.
[6] Head, R. M., "Investigation of Spontaneous Condensation Phenomena," Ph.D. thesis, 1949, California Inst. of Technology, Pasadena, Calif.
[7] Hermann, K. O. T. and Melnik, W. L., "Aerodynamic and Heat Transfer Characteristics of Basic Bodies in Hypersonic Flow of Air and of Combustion Gas Mixtures," TDR-62-89, 1962, Arnold Engineering Development Center, Tullahoma, Tenn.
[8] Fay, J. A. and Riddell, F. R., "Theory of Stagnation Point Heat Transfer in Dissociated Air," *Journal of the Aerospace Sciences*, Vol. 25, No. 2, Feb. 1958, pp. 73–85, 121.
[9] Stallings, R. L., Jr., and Howell, D. T., "Experimental Pressure Distribution for a Family of Blunt Bodies at Mach Numbers from 2.49 to 4.63 and Angles of Attack from 0° to 15°," TN D-5392, Aug. 1969, NASA.
[10] Weinstein, I., "Heat Transfer and Pressure Distributions on a Hemisphere-Cylinder and a Bluff-Afterbody Model in Methane-Air Combustion Products and Air," TN D-1503, 1962, NASA.
[11] Baer, A. L., "Pressure Distributions on a Hemisphere Cylinder at Supersonic and Hypersonic Mach Numbers," TN-61-96, U.S. Air Force, Aug. 1961, Arnold Engineering Development Center, Tullahoma, Tenn.
[12] Lomax, H. and Inuoye, M. "Numerical Analysis of Flow Properties about Blunt Bodies Moving at Supersonic Speeds in an Equilibrium Gas," TR R-204, July 1964, NASA.
[13] Kemp, N. H., Rose, P. H., and Detra, R. W., "Laminar Heat Transfer Around Blunt Bodies in Dissociated Air," *Journal of the Aerospace Sciences*, Vol. 26, No. 7, July 1959, pp. 421–430.
[14] Hunt, L., "Aerodynamic Force and Moment Characteristics of Spheres and Cones at Mach 7.0 in Methane-Air Combustion Products," TN D-2801, 1965, NASA.
[15] Hodges, A. J., "The Drag Coefficient of Very High Velocity Spheres," *Journal of the Aeronautical Sciences*, Vol. 24. No. 10, Oct. 1957, pp. 755–758.
[16] Penland, J. A., "Aerodynamic Characteristics of a Circular Cylinder at Mach Number 6.86 and Angles of Attack up to 90°," TN 3861, 1957, NACA.
[17] Kinslow, Max and Potter, J. L., "The Drag of Spheres in Rarefied Hypervelocity Flow," TDR-62-205, U.S. Air Force, Dec. 1962, Arnold Engineering Development Center, Tullahoma, Tenn.
[18] Aroesty, J., "Sphere Drag in a Low Density Supersonic Flow," Rept. HE-150-192, Contract N-onr.-222 45, Jan. 3, 1962, Inst. Engineering Research, University of California, Berkeley, Calif.
[19] Ladson, C. L. and Blackstock, T. A., "Air-Helium Simulation of the Aerodynamic Force Coefficients of Cones at Hypersonic Speeds," TN D-1473, 1962, NASA.
[20] Penland, J. A., "A study of the Stability and Location of the Center of Pressure on Sharp, Right Circular Cones at Hypersonic Speeds," TN D-2283, 1964, NASA.
[21] Merz, G. H. and Pritts, O. R., "Static Force Tests at Mach 8 of Sharp and Blunt 20-Deg Half-Angle Cones and a Blunt 70-Deg Swept Delta Wing," TDR-62-187, April 1962, U.S. Air Force, Arnold Engineering Development Center, Tullahoma, Tenn.
[22] Schueler, C. J., "Lift, Drag, and Pitching Moment Characteristics of AGARD Calibration Models A and B at Mach Numbers 3.98 and 4.98," TN 57-9, May 1957, Arnold Engineering Development Center, Tullahoma, Tenn.
[23] Coats, J. D., "Force Tests of an AGARD Calibration Model B at $M = 2.5$ to 6.0," TN-60-182, Oct. 1960, Arnold Engineering Development Center, Tullahoma, Tenn.
[24] Kayser, L. D. and Fitch, C. R., "Force and Pressure Tests of an AGARD Calibration Model B at a Mach Number of 8," TN-60-34, July 1960, Arnold Engineering Development Center, Tullahoma, Tenn.
[25] Schueler, C. J. and Strike, W. T., "Calibration of a 40-Inch Continuous Flow Tunnel at Mach Numbers 1.5 to 6," TN-59-136, Arnold Engineering Development Center, Tullahoma, Tenn.
[26] Douglas, D. W. and Martin, R. E., "An Investigation of the Lift, Drag, and Pitching-Moment Characteristics of the AGARD Calibration Model B at Mach Numbers 1.65 to 5.00 in the 20-Inch Supersonic Wind Tunnel," Rept. 20-129, Sept. 1959, Jet Propulsion Lab. California Inst. of Technology, Pasadena, Calif.
[27] Milillo, J. and Chevalier, H. L., "Test Results of the AGARD Calibration Model B and a Modified AGARD Model C in the AEDC Transonic Model Tunnel" TN-57-6, May 1957, Arnold Engineering Development Center, Tullahoma, Tenn.
[28] Milillo, J. R., "Transonic Tests of an AGARD Model B and a Modified Model C at 0.01 Percent Blockage," TN-58-48, Aug. 1958, Arnold Engineering Development Center, Tullahoma, Tenn.
[29] Mitchell, J. L., "Rocket Model Investigation of the AGARD Model B Configuration by the NACA Langley Laboratory," *A Review of Measurements on AGARD Calibration Models*, AGARDograph 64, Nov. 1961.
[30] Broom, A. F., Jr., "Investigation of Lift, Drag and Pitching Moment of a 60° Delta-Wing-Body Combination (AGARD Calibration Model B) in the Langley 9-Inch Supersonic Tunnel," TN-3300, Sept. 1954, NACA.
[31] "Wind Tunnel Calibration Models, AGARD Specification 2," Sept. 1958, AGARD.